



**COMPUMAG  
2009**



Florianópolis, Brazil

Proceedings of the  
**17<sup>th</sup> Conference on the Computation of  
Electromagnetic Fields**

November, 22<sup>nd</sup> – 26<sup>th</sup>  
Florianópolis, Brazil

ORGANISATION:



SPONSORING:



<b>PC6.20</b> .....	795
Novel Modeling of Flux-barriers in Interior-type PM Synchronous Motor For Pulsation Torque Reduction: Part I. Various Flux-barrier Designs	
<i>Liang Fang, Jeong-Jong Lee, Jung-Pyo Hong</i>	
<b>PC6.21</b> .....	797
Parametric Finite Element Analyses of a Permanent Magnet Synchronous Machine with an External Rotor	
<i>Erich Schmidt, Marko Susic</i>	
<b>PC6.22</b> .....	799
2D Exact Analytical Solution of Open Circuit Magnetic Field in Slotted Surface Mounted PM Radial Flux Synchronous Machines	
<i>Yacine Amara, Jacques Raharijaona, Georges Barakat</i>	
<b>PC6.23</b> .....	801
Quasistatic Electromagnetic Field Computation by Conformal Mapping in Permanent Magnet Synchronous Machines	
<i>Martin Hafner, David Franck, Kay Hameyer</i>	
<b>PC6.24</b> .....	803
Calculation of Inductances in Intercell Transformers by 2D FEM simulation	
<i>Bernardo Cougo, Thierry Meynard, François Forest, Eric Labouré</i>	

### Session PC7: Numerical Techniques III

13:30-15:00 – Room: Poster Session Room II

<b>PC7.1</b> .....	805
Study on Analysis Method for Ferrofluid	
<i>Yu Okaue, Gaku Yoshikawa, Fumikazu Miyasaka, Katuhiro Hirata</i>	
<b>PC7.2</b> .....	807
Isogeometric analysis for electromagnetic problems	
<i>Annalisa Buffa, Rafael Vázquez</i>	
<b>PC7.3</b> .....	809
Nonoverlapping and overlapping decomposition methods in 3D BEM multilayered model for Optical Tomography	
<i>Tomasz Marek Grzywacz, Jan Sikora</i>	

# Flexible Flux-barrier Designs For Torque Pulsation Reduction in Interior-type Permanent Magnet Synchronous Motor

Liang Fang<sup>1</sup>, Jeong-Jung Lee<sup>1</sup>, Jung-Pyo Hong<sup>1</sup>, Myung-Ryul Choi<sup>2</sup>

<sup>1</sup>Department of Automotive Engineering, Hanyang University, Seoul 133-791, Korea

<sup>2</sup>School of EECS, Hanyang University, Ansan, Gyunggi-do 426-791, Korea

The flexible flux-barrier designs for torque pulsation reduction in an interior permanent magnet synchronous motor (IPMSM) are investigated in this paper. A prototype conventional single-layer IPMSM model, a popular double-layer IPMSM model and a proposed novel double-barrier IPMSM model are built in the same stator/rotor frame. The novel flux-barrier design having beneficial attributes of simplicity of single-layer IPM in manufacture and flexible double pair of flux-barriers in rotor design is emphasized. The geometries of buried flux-barriers in each IPMSM models are optimized with the help of response surface methodology (RSM) for minimizing both torque ripple and cogging torque. Finite element analysis (FEA) and test results well confirmed the presented analysis.

*Index Terms*—FEA, IPMSM, RSM, single-layer/double-layer/novel double-barrier IPM design, torque pulsation reduction.

## I. INTRODUCTION

THE INTERIOR permanent magnet synchronous motors (IPMSM) are widely used in home application, industrial, and electric and hybrid vehicle (HEV) propulsion, due to their high efficiency, high torque density and wide speed range [1]. However, the significant torque pulsation is an inherent drawback of IPMSM, which results in mechanical resonance, vibration, acoustic noise and damage to drive component [2]. Therefore, the torque pulsation reduction design is always very crucial for most applications which require smooth motor running. Many papers dealt with this problem, and proposed some effective approaches, such as slot-opening design.

In this paper, the torque pulsation reduction in IPMSM is realized by properly designing the buried flux-barrier structure inside rotor to minimize pulsation components of output torque. The flexibility and effectiveness of different flux-barrier designs on torque pulsation reduction are examined.

The conventional single-layer IPMSMs have only one pair of flux-barriers with each single PM piece buried in rotor iron, which benefits to be easily manufactured. And the popular double-layer IPMSMs are attractive since their variable double pairs of flux-barriers can be utilized in the IPM rotor design. In addition, this paper proposes a novel IPMSM model design features double flux-barrier created with each single-layer IPM, which obviously have beneficial attribute of the flexible double pair of flux-barrier in rotor design similar to double-layer design IPMSM, and the simplicity and low-costing in manufacture close to single-layer design IPMSM.

With the help of response surface methodology (RSM) technique, the geometries of each mentioned flux-barrier designs are optimized for reducing torque pulsation in IPMSM. The finite element analysis (FEA) coupled with equivalent circuit method is used to analyze IPMSM torque performance and examine the effectiveness of each flux-barrier design. The experiment method is applied to confirm the validity of the presented flux-barrier design approach in IPMSM.

## II. TORQUE PULSATION REDUCTION AND FLEXIBLE BURIED FLUX-BARRIER MODELING

### *Torque Pulsation Reduction Method*

The torque pulsation reduction design usually focus on the torque ripple of output torque, which caused by the interaction of rotor field and stator current, as well as the cogging torque, arises from the interaction of rotor flux and slotted core structure. Therefore, the obvious effective approach to reduce torque pulsation is to improve the magnetic field in air-gap, which always realized by decreasing the total harmonic distortion (THD) of back electromotive force (Back-EMF), and altering the distribution of PM flux out of rotor surface [3].

### *Flexible Flux-barrier Designs*

The effectiveness of various flux-barrier designs on the torque pulsation reduction in IPMSM is examined in this study. Base on a prototype conventional single-layer IPMSM model, as Fig. 1 gives, a double-layer IPMSM model is built by splitting the same PM segment into double equithickness pieces under the same design frame, as TABLE I lists. It creates two pairs of separated flux-barrier, which benefit to effectively distribute the magnetic flux crossing into air-gap to form a sinusoidal magnetic field, as Fig. 2(a) illustrates. On the other hand, it should be aware that the double-layer IPM design will unavoidably increase the manufacture cost and difficulties, and may cause PM irreversible demagnetization in the thin PM pieces under over large armature current.

TABLE I  
DIMENSION AND SPECIFICATIONS OF PROTOTYPE IPMSM

Items	Value	Unit
Stator outer diameter	117.2	mm
Rotor outer diameter	70.8	mm
Stack length	15	mm
Air-gap length	0.6	mm
Br (@20~25°C)	1.22~1.28	T
Maximum terminal voltage	98.6	V
Rated output power	2	kW
Maximum current	17	A <sub>rms</sub>
Base speed	3500	rpm

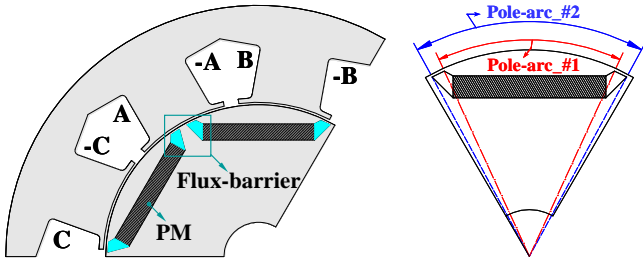


Fig. 1. Configuration of conventional single-layer IPMSM model.

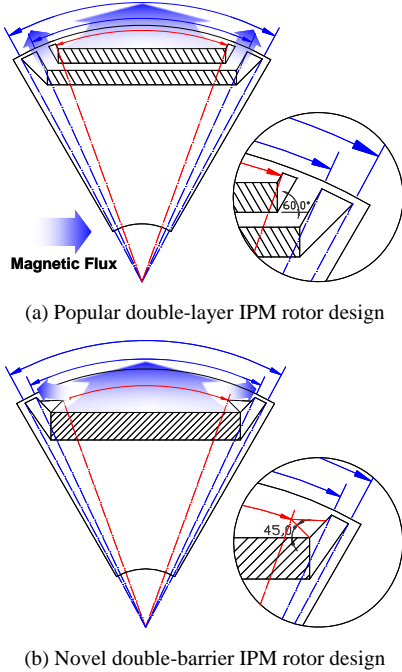


Fig. 2. Double pairs of flux-barrier designs based on single-layer IPM rotor

In this paper, a novel double-barrier IPM rotor model is proposed, as Fig. 2(b) illustrates. The single-layer IPM has two pairs of connected flux-barrier, by which the shunting action of PM magnetic flux is also realized effectively. In essence, it is similar to the feature of double-layer IPM rotor design, but decreased the cost and manufacturing difficulties.

### III. IPMSM CHARACTERISTIC ANALYSIS

In this paper, the torque performance of IPMSM is analyzed by performing equivalent circuit method (ECM), which based on the machine parameters calculated by FEA, such as  $d$ -,  $q$ -axis inductances and fundamental component of Back-EMF.

In a  $d$ - $q$  reference frame, a widely proved equivalent circuit with iron loss consideration is built, as Fig. 3 illustrates [4]. Correspondingly, the IPMSM mathematical model is obtained as voltages and currents equations (1) and (2), and the output torque characteristic is expressed as equations (3).

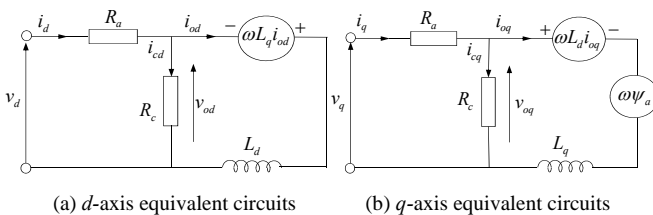


Fig. 3. Equivalent circuit of IPMSM

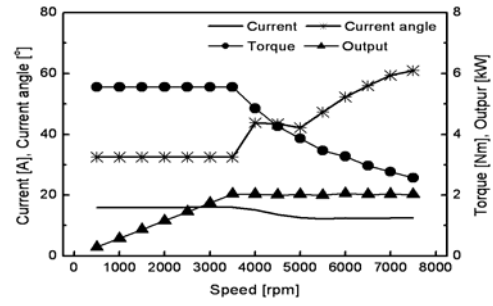


Fig. 4. Speed versus torque and output performance of IPMSM by ECM.

$$\begin{bmatrix} v_d \\ v_q \end{bmatrix} = R_a \begin{bmatrix} i_{od} \\ i_{oq} \end{bmatrix} + \left(1 + \frac{R_a}{R_c}\right) \begin{bmatrix} v_{od} \\ v_{oq} \end{bmatrix} + p \begin{bmatrix} L_d & 0 \\ 0 & L_q \end{bmatrix} \begin{bmatrix} i_{od} \\ i_{oq} \end{bmatrix} \quad (1)$$

$$\begin{bmatrix} v_{od} \\ v_{oq} \end{bmatrix} = \begin{bmatrix} 0 & -\omega L_d \\ \omega L_d & 0 \end{bmatrix} \begin{bmatrix} i_{od} \\ i_{oq} \end{bmatrix} + \begin{bmatrix} 0 \\ \omega \psi_a \end{bmatrix} \quad (2)$$

$$\begin{aligned} T &= P_n [\psi_a i_a \cos \beta + (L_d - L_q) i_d i_q] \\ &= P_n [\psi_a I_a \cos \beta + \frac{1}{2} (L_d - L_q) I_a^2 \sin 2\beta] \end{aligned} \quad (3)$$

where  $i_d$ ,  $i_q$ :  $d$ ,  $q$  components of armature current;  $v_d$ ,  $v_q$ :  $d$ ,  $q$  components of terminal voltage;  $\psi_a$ :  $\sqrt{3/2} \psi_f$ ;  $\psi_f$ : maximum flux linkage of permanent magnet;  $R_a$ : armature winding resistance;  $R_c$ : iron loss equivalent resistance,  $L_d$ ,  $L_q$ : inductance along  $d$ -,  $q$ -axis;  $p = d/dt$ ;  $P_n$ : number of pole pairs.

By performing the above  $d$ -,  $q$ -axis equivalent circuits, the torque performance of IPMSM can be predicted quickly. In the simulation, the limitation of armature current and terminal voltage must be considered. From the torque equation (3), the input armature current  $I_a$  and current phase angle  $\beta$  are necessary to predict torque characteristic at each state.

The entire speed range operation considering the control conditions is acquired in the following manner. In the anterior region of base speed, maximum torque per ampere control is employed, and flux weakening control is applied in the posterior region. Fig. 4 shows the results of speed versus torque and output performance, also the input current and its phase angle. Therefore, the torque characteristic at any speed operation can be calculated by FEA. In this study, the rated torque operated at base speed 3500 [rpm] is focused, that its torque pulsation is desired to be reduced.

### IV. OPTIMAL SHAPE DESIGN OF FLUX-BARRIER

The IPM rotor inner geometry design is very complex owing to many design factors. Thus, a well-known efficient technique, RSM is adopted in each type flux-barrier design.

TABLE II  
EXPERIMENT RANGES OF DESIGN VARIABLES FOR OPTIMIZATION BY RSM

Presented Analysis IPMSM Model	Pole-arc #0 [Outer layer]	Pole-arc #1 [Inner layer]	Pole-arc #2 [Inner layer]
Single-layer design		41° ~ 48°	54.2° ~ 59.2°
Double-layer design	35.4° ~ 41°	46° ~ 52°	54.2° ~ 59.2°
Double-barrier design	35.4° ~ 41°	46° ~ 52°	54.2° ~ 59.2°

\* Outer layer: the upper PM layer closing to rotor surface.

RSM is a set of statistical and mathematical techniques to find the “best fitted” response of the physical system through experiment or simulation [5]. In this paper, the RSM is applied for searching the optimal structure of each flux-barrier design in order to minimize the torque pulsation of IPMSM.

For investigating the influence of each flux-barriers design on torque pulsation reduction, only the magnet pole-arcs, which defined by flux-barriers structure variation, are chosen as design variables in RSM optimization. For example, the single-layer IPM pole-arc is described in term of pole-arc #1 and #2, with considering the rib region, as shown in Fig. 1

Here, the optimal design of double-layer IPM rotor model by using RSM is taken for example. For decreasing the design difficulty, the non-significant design variable can be fixed to be a proper constant value. There are three variables are used to describe the two pairs of flux-barrier designs, as Fig. 2(a) arrows show. Table II lists the experiment range of each design variables [Pole-arc\_#0, Pole-arc\_#1 and Pole-arc\_#2] in RSM, and the simulation models are built according to the full factorial combinations of design variables. With the given three design variables, fifteen different models are required to be analyzed, as Table III lists. Each analysis model is analyzed.

In RSM optimization, the goal values of design objectives: toque ripple at rated operation and cogging torque amplitude (peak-peak value), in addition THD of Back-EMF are decided firstly. And the simulation conditions, output torque and power constraints are given as followings:

- Design objectives:

$$Y_{\text{Trip}} \leq 10.0[\%], \quad Y_{\text{CT(p-p)}} \leq 0.16[\text{Nm}], \quad Y_{\text{THD}} \leq 4.0[\%]$$

- Subject to:

$$Y_{\text{Tave}} \geq 5.5[\text{Nm}], \quad \text{Output power} \geq 2[\text{kW}]$$

TABLE III  
DESIGN VARIABLES AND RESPONSES OF RSM SIMULATION

P-arc_#0	P-arc_#1	P-arc_#2	$Y_{\text{Trip}}$	$Y_{\text{CT(p-p)}}$	$Y_{\text{THD}}$
36.5°	47.35°	55.15°	15.86	0.055	3.05
39.8°	47.35°	55.15°	15.23	0.156	4.04
36.5°	50.8°	55.15°	12.57	0.088	3.32
39.8°	50.8°	55.15°	12.50	0.090	3.96
36.5°	47.35°	58.15°	14.60	0.055	3.61
39.8°	47.35°	58.15°	13.51	0.150	4.57
36.5°	50.8°	58.15°	10.54	0.087	4.84
39.8°	50.8°	58.15°	9.56	0.084	5.39
35.4°	49.08°	56.65°	10.75	0.176	4.08
41.0°	49.08°	56.65°	11.07	0.140	4.41
38.15°	46.0°	56.65°	14.41	0.087	5.01
38.15°	52.0°	56.65°	10.41	0.054	4.38
38.15°	49.08°	54.2°	15.83	0.092	3.55
38.15°	49.08°	59.2°	14.23	0.087	5.00
38.15°	49.08°	56.65°	12.89	0.091	4.22

\* “ ” : according to the variables experiment ranges as TABLE I lists.

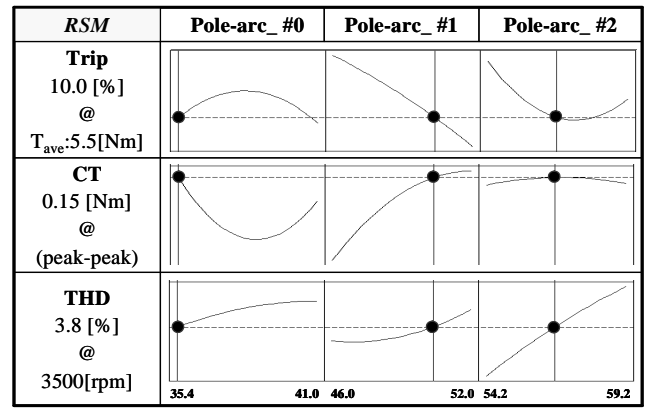


Fig. 5. Responses of design objectives with design variables in RSM

TABLE IV  
OPTIMIZED DESIGN VARIABLES OF FLUX-BARRIERS BY RSM

Optimal Model	Pole-arc #0	Pole-arc #1	Pole-arc #2
Single-layer design		46.0°	58.0°
Double-layer design	35.4°	50.4°	56.6°
Double-barrier design	36.0°	52.0°	59.0°

The responses of torque ripple, cogging torque and THD of Back-EMF according to each design variables are displayed in Fig.5. Since the minimum torque ripple is preferential, then the cogging torque and THD, therefore, the “fittest” points are selected as “broken lines” show. All the required design objective values are satisfied as predicted in RSM. And then, the optimal double-layer design IPMSM model can be built by using the corresponding design variables in RSM.

## V. RESULT AND DISCUSS

With the given design variables, the other two flux-barrier designs in IPMSM models are optimized following the same process of double-layer IPMSM optimization. The “optimal” results predicted in RSM simulation are confirmed by FEA. Therefore, each of the optimized IPMSM models are built with the “fittest value” of design variables, as TABLE IV lists.

Also, the experiment method is applied to verify the validity of calculated IPMSM characteristics obtained by the FEA coupled with ECM. Then, by using proved analysis approach, torque ripple, cogging torque and Back-EMF characteristics of the three optimized IPMSM models are compared for examining the effectiveness of these various flux-barrier designs on torque pulsation reduction in IPMSM.

### A. Test of Double-layer Design IPMSM

The optimized double-layer design IPMSM is fabricated and tested, as Fig. 6 shows. Firstly, its torque ripple at rated operation (3500rpm) is tested by inputting current 15.3[Arms] with phase angle  $\beta=32.5^\circ$  determined by the presented equivalent circuit analysis. It is found that the tested result 7.8[%] is smaller than the FEA result 10.0[%], as Fig. 7 shows. The error is thought caused by the influence of the reduction gear inertial. And the measured cogging torque and Back-EMF characteristics show good agreement with FEA results, as Fig. 8 and Fig. 9 show. The slightly different may be caused by manufacturing.

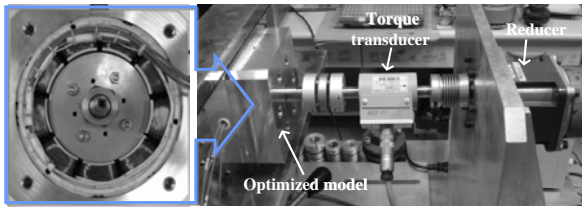
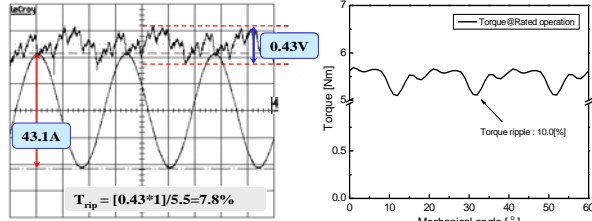


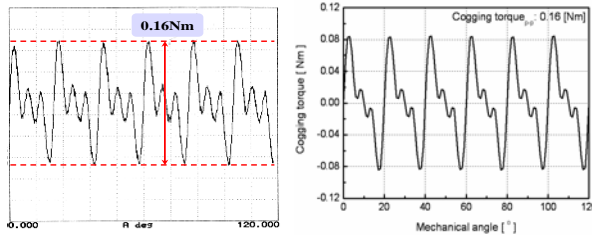
Fig. 6. Fabricated double-layer IPMSM and torque performance test.



(a) Test result [1V indicates 1Nm]

(b) FEA result

Fig. 7. Torque ripple of double-layer IPMSM @ Rated torque=5.5[Nm]



(a) Test result

(b) FEA result

Fig. 8. Cogging torque results of double-layer IPMSM.

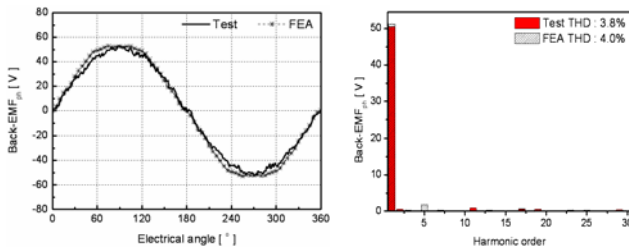
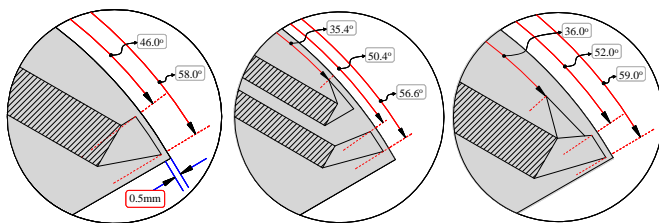


Fig. 9. No-load Back-EMF and THD results @ at 3500rpm

**B. Torque Ripple and Cogging Torque Reduction Analysis**

Fig. 10 illustrates the geometries of three optimized flux-barriers structure in each IPM rotor core. The rib region keeps 0.5[mm] margin for considering mechanical robustness. Since the different extent of flux-barrier designs change the flux path inside rotor core, the double-layer design and the proposed novel double-barrier design are effective on reducing torque ripple and cogging torque of single-layer design IPMSM, as Fig. 11 and Fig 12 show respectively. Obviously, the novel double-barrier design is practicable to replace the double-layer design for improving torque performance of IPMSM.



(a) Single-layer design (b) Double-layer design (c) Double-barrier design

Fig. 10. Optimized flux-barriers designs in each IPMSM analysis model

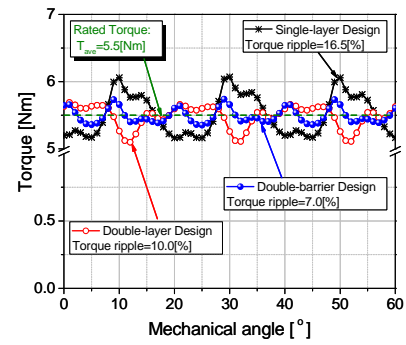


Fig. 11. Torque ripple reduction comparison by FEA

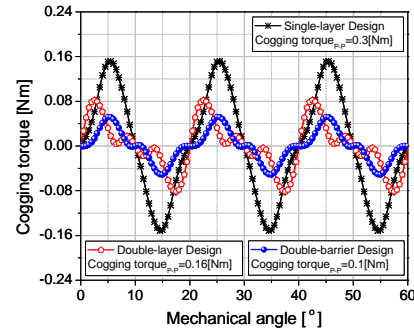


Fig. 12. Cogging torque reduction comparison by FEA

**VI. CONCLUSION**

Torque pulsation reduction in IPMSM by optimizing the flux-barrier structures in rotor design was presented in this paper. Beside a popular double-layer design IPMSM model, a novel double-barrier IPMSM model, featuring as each single-layer PM coupled with double pairs of flux-barrier, was proposed to improve the torque performance of single-layer design IPMSM model. The significant effectiveness of double-layer design and novel double-barrier design on torque ripple and cogging torque reduction is well verified by FEA and test results. In conclusion, the proper flux-barrier structure as an effective design approach for reducing torque pulsation is confirmed. The novel double-barrier design has attributes of flexible flux-barrier in design and simplest PM insertion in manufacture has been proved.

**REFERENCES**

- [1] Nicole Bianchi, Thomas M. Jahns, "Design, Analysis, and Control of Interior PM synchronous Machines", *IEEE-IAS Electrical Machines Committee*.
- [2] R. Islam, I. Husain, A. Fardoun, K. McLaughlin, "Permanent-Magnet Synchronous Motor Magnet Designs With Skewing for Torque Ripple and Cogging Torque Reduction," *IEEE Transaction on Industry Applications*, vol. 45, no. 1, January/February 2009.
- [3] Gyu-Hong Kang, Jung-Pyo Hong, Gyu-Tak Kim, "Analysis of Cogging Torque in Interior Permanent Magnet Motor by Analytical Method," *KIEE International Transaction on Electrical Machinery and Energy Conversion Systems*, v.11B, no.2, pp.1-8, June 2006.
- [4] Liang Fang; Jae-woo Jung; Jung-Pyo Hong; Jung-Ho Lee, "Study on High-Efficiency Performance in Interior Permanent-Magnet Synchronous Motor With Double-Layer PM Design," *IEEE Trans. Magn.*, vol. 44, Issue 11, Part 2, Nov. 2008.
- [5] L. Qinghua, M. A. Jabbar, and M. Khambadkone, "Response surface methodology based design optimization of interior permanent magnet synchronous motors for wide-speed operation," in *Proc. PEMD*, vol. 2, pp. 546-551, March/April 2004